Fig. S1

(A)

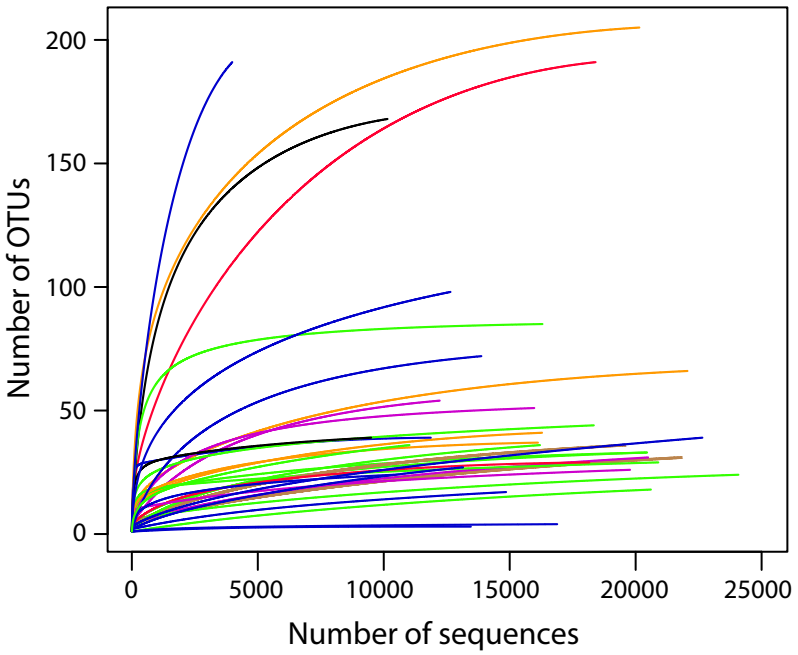

Sample (Species / Nest ID)	N sequences	N OTUs
Megalomyrmex wettereri RMMA100604-08	20147	205
Sericomyrmex amabilis JOA120528-05	3987	191
Cyphomyrmex cornutus RMMA030213-09	18409	191
Fungus garden JOA120528-02	10149	168
Sericomyrmex amabilis RMMA120514-01	12648	98
Megalomyrmex wallacei RMMA110328-05	16300	85
Sericomyrmex amabilis AI110511-05	13874	72
Cyphomyrmex longiscapus JL110513-03	22056	66
Cyphomyrmex costatus RMMA110521-04	12221	54
Megalomyrmex mondaboroides RMMA110521-04	15975	51
Megalomyrmex staudingeri RMMA040609-05	18338	44
Cyphomyrmex longiscapus RMMA110523-06	16284	41
Fungus garden JOA120604-03	9051	39
Megalomyrmex symmetochus RMMA120514-01	11867	39
Sericomyrmex amabilis JOA120525-01	22649	39
Megalomyrmex wettereri RMMA100629-06	16121	37
Megalomyrmex longinoi RMMA100625-01	11022	36
Megalomyrmex modestus RMMA110328-09	16201	36
Trachymyrmex zeteki RMMA050727-06	19611	36
Megalomyrmex incisus RMMA060311-15	20426	33
Megalomyrmex glaesarius RMMA060314-03	20454	33
Cyphomyrmex costatus RMMA100624-18	20496	31
Megalomyrmex adamsae RMMA050727-06	21862	31
Megalomyrmex mondabora RMMA030213-09	18159	29
Megalomyrmex incisus BeB000836-2	20899	29
Sericomyrmex amabilis JOA120604-03	13148	27
Megalomyrmex silvestrii GBM.sil2010	19777	26
Sericomyrmex amabilis JOA120528-02	10404	24
Megalomyrmex foreli RMMA110323-05	24079	24
Megalomyrmex milenae BA130514-18	20604	18
Megalomyrmex symmetochus AI110511-05	14857	17
Megalomyrmex symmetochus JOA120604-03	16885	4
Megalomyrmex symmetochus JOA120528-05	13456	3

(B)

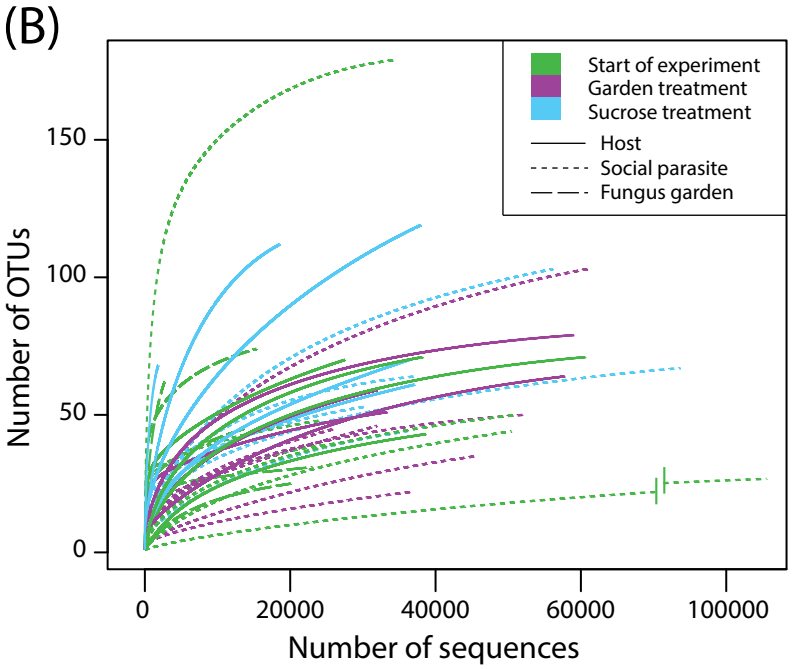

Sample (Species / Nest ID)	N sequences	N OTUs
Megalomyrmex mondaboroides RMMA110521-04	34472	179
Sericomyrmex amabilis AI110515-06	37959	119
Sericomyrmex amabilis RMMA120514-01	18569	112
Megalomyrmex symmetochus RMMA120514-01	56147	103
Megalomyrmex symmetochus JOA120604-01	60881	103
Sericomyrmex amabilis JOA120604-01	59063	79
Fungus garden RMMA100629-06	15385	74
Sericomyrmex amabilis JOA120604-01	60613	71
Sericomyrmex amabilis RMMA120514-01	38231	71
Sericomyrmex amabilis JOA120604-01	36386	70
Sericomyrmex amabilis AI110515-06	27541	70
Sericomyrmex amabilis JOA120516-01	1839	68
Megalomyrmex symmetochus JOA120604-01	73705	67
Megalomyrmex symmetochus JOA120516-01	37294	64
Sericomyrmex amabilis RMMA120514-01	57783	64
Fungus garden JOA120604-01	2719	62
Megalomyrmex mondaboroides RMMA110521-04	37129	61
Sericomyrmex amabilis JOA120516-01	31949	59
Megalomyrmex wettereri RMMA100629-06	30336	53
Sericomyrmex amabilis AI110515-06	33339	51
Megalomyrmex symmetochus JOA120516-01	52055	50
Megalomyrmex symmetochus RMMA120514-01	51140	50
Megalomyrmex symmetochus JOA120604-01	24309	48
Megalomyrmex mondaboroides RMMA110521-04	31961	46
Fungus garden RMMA110521-04	13706	45
Megalomyrmex wettereri RMMA100629-06	26172	45
Megalomyrmex symmetochus AI110515-06	36024	44
Megalomyrmex wettereri RMMA100629-06	50452	44
Sericomyrmex amabilis JOA120516-01	38662	43
Megalomyrmex symmetochus AI110515-06	27658	40
Megalomyrmex symmetochus RMMA120514-01	45600	35
Fungus garden RMMA120514-01	3556	33
Fungus garden JOA120516-01	23071	31
Megalomyrmex symmetochus JOA120516-01	128170	29
Fungus garden AI110515-06	20085	25
Megalomyrmex symmetochus AI110515-06	36675	22

Fig. S1 Rarefaction curves of tag-encoded FLX 454 pyrosequencing samples (A) and Illumina MiSeq diet experiment samples (B). Plots show the number of OTUs as a function of the simulated sequencing effort, with sample IDs and number of assigned reads and OTUs per sample given towards the right of the plots. Samples from (A) are colored based on the different specific host-parasite associations and free-living *Megalomyrmex* as in Fig. 1 with the two fungus gardens in black, while samples from (B) are colored by experimental treatment group.

Fig. S2

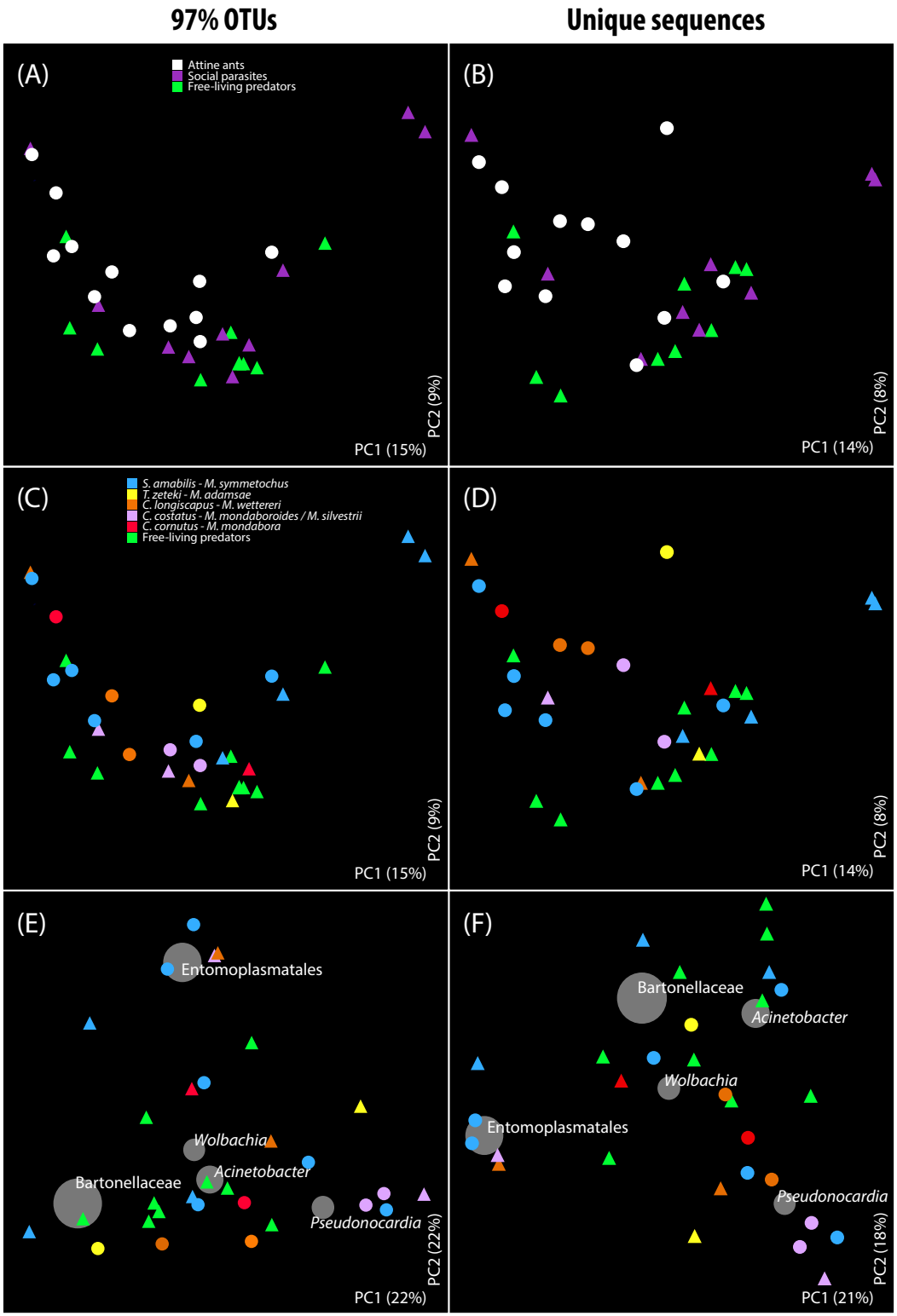
97% OTUs
Unique sequences
(A)
Attine ants
Social parasites
Free-living predators
PC2 (9%)
PC1 (15%)
(B)
PC2 (8%)
PC1 (14%)
(C)
S. amabilis - M. symmetochus
T. zeteki - M. adamsae
C. longiscapus - M. wettereri
C. costatus - M. mondaboroides / M. silvestrii
C. cornutus - M. mondabora
Free-living predators
PC2 (9%)
PC1 (15%)
(D)
PC2 (8%)
PC1 (14%)
(E)
Entomoplasmatales
Wolbachia
Acinetobacter
Bartonellaceae
Pseudonocardia
PC2 (22%)
PC1 (22%)
(F)
Bartonellaceae
Acinetobacter
Wolbachia
Entomoplasmatales
Pseudonocardia
PC2 (18%)
PC1 (21%)

Fig. S2 Principal Coordinates Analyses (PCoA) of unweighted UniFrac metrics based on 97% OTUs (A and C) or unique sequences (B and D) and PCoA bi-plots of weighted UniFrac metrics based on 97% OTUs (E) or unique sequences (F). *Megalomyrmex* samples are shown as triangles and attine host samples as circles. The A, B, C and D plots are identical to the plots given in Fig. 2, but have colored symbols to illustrate how samples are assigned to the different categories. Panels A and B are colored by hosts (white), social parasites (purple) and free-living predators (green), while, as in Fig. 1, symbols in panels C, D, E and F are colored by the five categories of associated hosts and social parasites, with the free-living *Megalomyrmex* predators being plotted in green as a sixth category. The positions of the triangles and circles are averages after 100 jackknife replications. The bi-plots (panels E and F) show the contribution of each of the five most abundant bacterial lineages (grey circles with diameters proportional to the mean relative abundance of the taxon across all samples) to the clustering patterns of ant samples.

Fig. S3

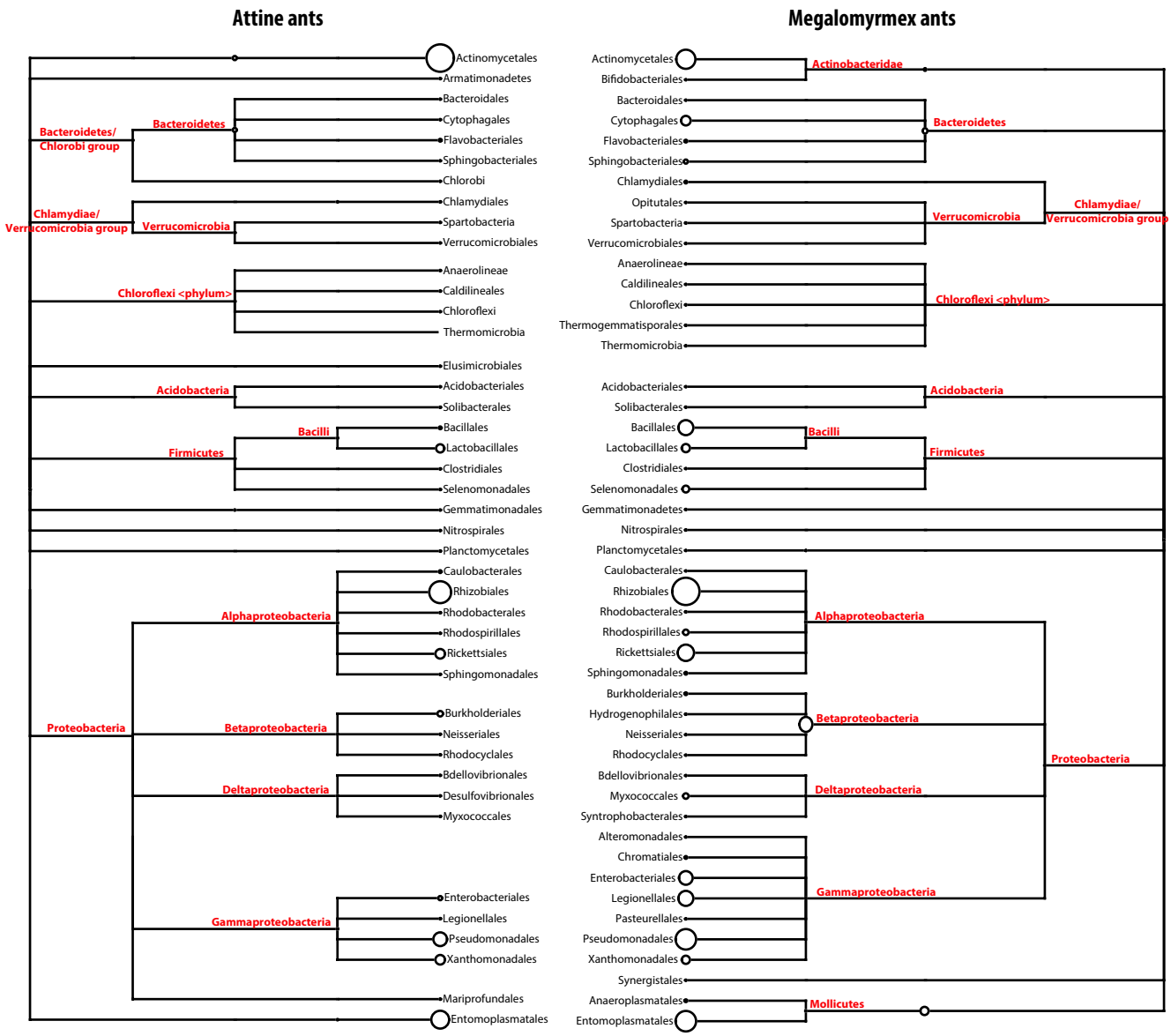
Attine ants
Megalomyrmex ants
Actinomycetales
Armatimonadetes
Bacteroidales
Cytophagales
Flavobacteriales
Sphingobacteriales
Bacteroidetes
Bacteroidetes/ Chlorobi group
Chlorobi
Chlamydiales
Spartobacteria
Verrucomicrobiales
Verrucomicrobia
Chlamydiae/ Verrucomicrobia group
Anaerolineae
Caldilineales
Chloroflexi
Thermomicrobia
Chloroflexi <phylum>
Elusimicrobiales
Acidobacteriales
Solibacterales
Acidobacteria
Bacillales
Lactobacillales
Clostridiales
Selenomonadales
Bacilli
Firmicutes
Gemmatimonadales
Nitrospirales
Planctomycetales
Caulobacterales
Rhizobiales
Rhodobacterales
Rhodospirillales
Rickettsiales
Sphingomonadales
Alphaproteobacteria
Burkholderiales
Neisseriales
Rhodocyclales
Betaproteobacteria
Bdellovibrionales
Desulfovibrionales
Myxococcales
Deltaproteobacteria
Proteobacteria
Enterobacteriales
Legionellales
Pseudomonadales
Xanthomonadales
Gammaproteobacteria
Mariprofundales
Entomoplasmatales
Actinomycetales
Bifidobacteriales
Actinobacteridae
Bacteroidales
Cytophagales
Flavobacteriales
Sphingobacteriales
Bacteroidetes
Chlamydiales
Opitutales
Spartobacteria
Verrucomicrobiales
Verrucomicrobia
Chlamydiae/ Verrucomicrobia group
Anaerolineae
Caldilineales
Chloroflexi
Thermogemmatisporales
Thermomicrobia
Chloroflexi <phylum>
Acidobacteriales
Solibacterales
Acidobacteria
Bacillales
Lactobacillales
Bacilli
Clostridiales
Selenomonadales
Firmicutes
Gemmatimonadales
Nitrospirales
Planctomycetales
Caulobacterales
Rhizobiales
Rhodobacterales
Rhodospirillales
Rickettsiales
Sphingomonadales
Alphaproteobacteria
Burkholderiales
Hydrogenophilales
Neisseriales
Rhodocyclales
Betaproteobacteria
Bdellovibrionales
Myxococcales
Syntrophobacterales
Deltaproteobacteria
Proteobacteria
Alteromonadales
Chromatiales
Enterobacteriales
Legionellales
Pasteurellales
Pseudomonadales
Xanthomonadales
Gammaproteobacteria
Synergistales
Anaeroplasmatales
Entomoplasmatales
Mollicutes

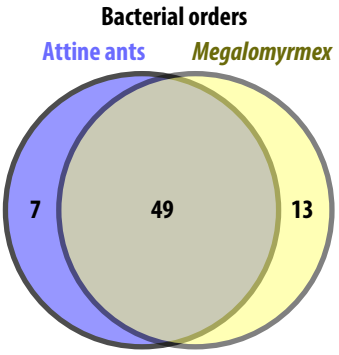
Bacterial orders
Attine ants
Megalomyrmex
7
49
13

Fig. S3 Phylogenetic trees of all 69 bacterial orders identified across attine and *Megalomyrmex* ants from the 454 16S rRNA pyrosequencing dataset. White circles at the tips of branches are proportional to the square-root of all the reads found in each order. The Venn diagram shows the proportion of unique and shared bacterial orders between the two ant lineages. Each bacterial order was identified from at least one sample of *Megalomyrmex* and/or attine ants.

Fig. S4

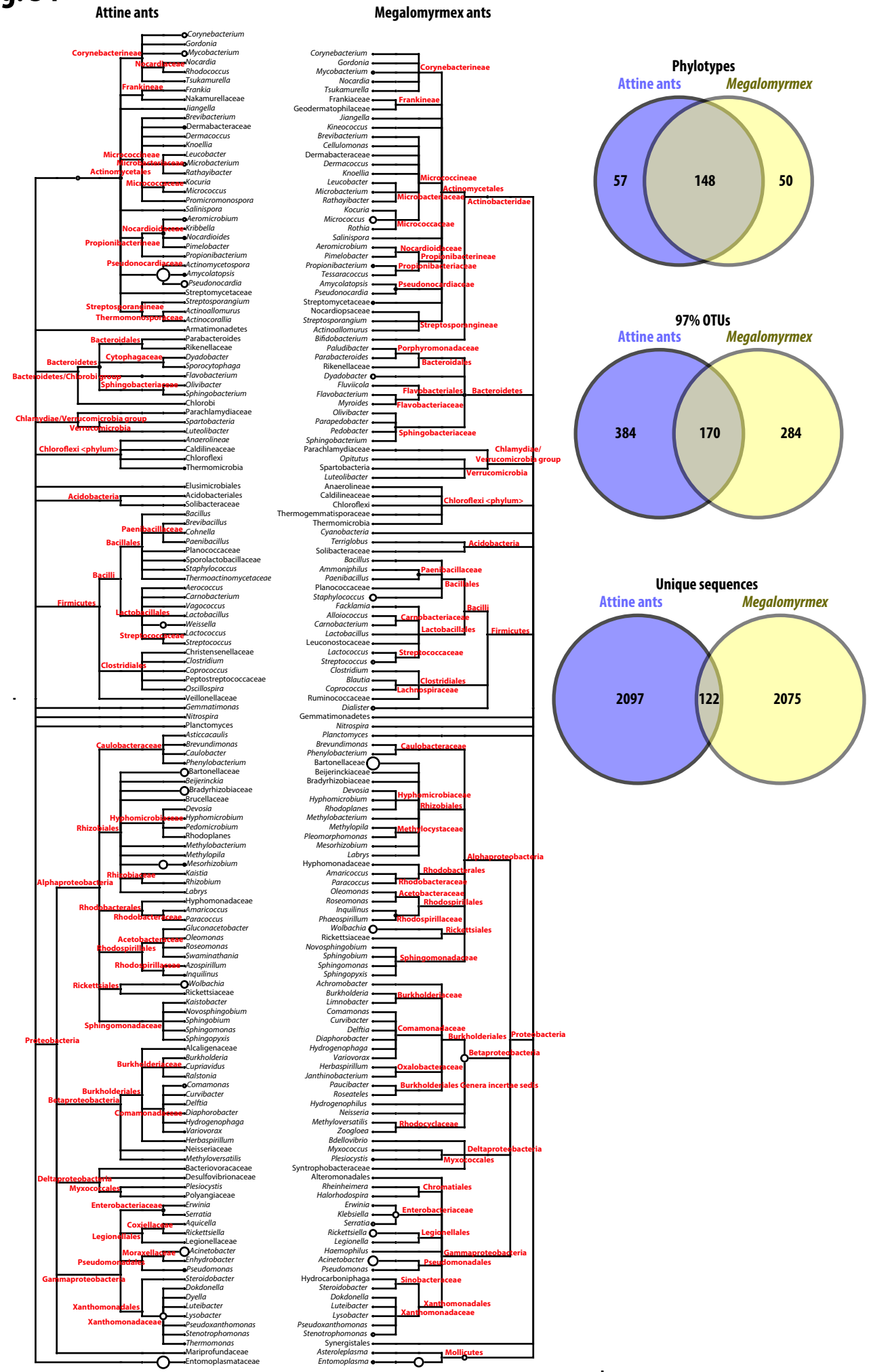
Attine ants
Megalomyrmex ants
Phylotypes
Attine ants
Megalomyrmex
57
148
50
97% OTUs
Attine ants
Megalomyrmex
384
170
284
Unique sequences
Attine ants
Megalomyrmex
2097
122
2075

Fig. S4 Phylogenetic trees of all 255 bacterial phylotypes identified across attine and *Megalomyrmex* ants from the 454 16S rRNA pyrosequencing dataset. White circles at the tips of branches are proportional to the square-root of all the reads found in each phylotype. Venn diagrams show the proportion of unique and shared bacterial phylotypes, 97% OTUs and unique sequences between the two ant lineages. Each phylotype, OTU or unique sequence was identified from at least one sample of *Megalomyrmex* and/or attine ants.

Fig. S5

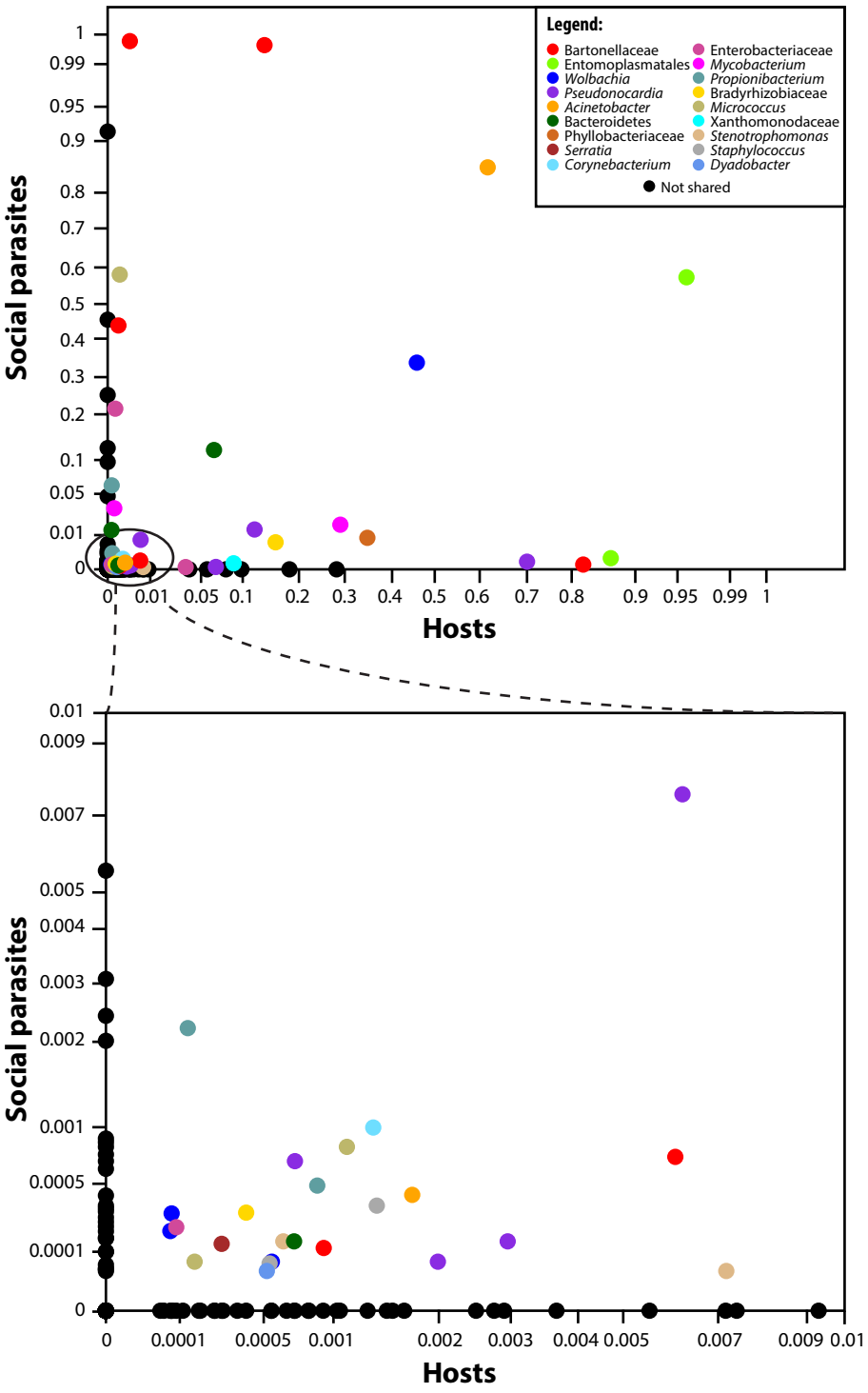
Legend:
Bartonellaceae
Entomoplasmatales
Wolbachia
Pseudonocardia
Acinetobacter
Bacteroidetes
Phyllobacteriaceae
Serratia
Corynebacterium
Enterobacteriaceae
Mycobacterium
Propionibacterium
Bradyrhizobiaceae
Micrococcus
Xanthomonodaceae
Stenotrophomonas
Staphylococcus
Dyadobacter
Not shared
Social parasites
Hosts
1
0.99
0.95
0.9
0.8
0.7
0.6
0.5
0.4
0.3
0.2
0.1
0.05
0.01
0
0.01
0.009
0.007
0.005
0.004
0.003
0.002
0.001
0.0005
0.0001
0
0.0001
0.0005
0.001
0.002
0.003
0.004
0.005
0.007
0.009
0.01

Fig. S5 Proportions of shared phylotypes in hosts and social parasites from joint nests as estimated from the 454 16S rRNA pyrosequencing dataset. Each dot combines the relative abundance in social parasites (y axes) and hosts (x axes) of a single phylotype in one of the eight nests from which hosts and parasites were collected jointly (H and P symbols next to pie charts in Fig. 3). Shared phylotypes are color-coded (cf. inset) and non-shared phylotypes are plotted in black. Note that the same phylotype can be shared in one nest but not in another and that there can be multiple dots with the same color, representing the same phylotype shared between hosts and parasites from different nests. Relative abundances are plotted on arcsine transformed scales to enhance separation between shared and non-shared phylotypes. Phylotypes that were infecting the ants only in trace amounts are shown in further detail in the lower plot.

Fig. S6

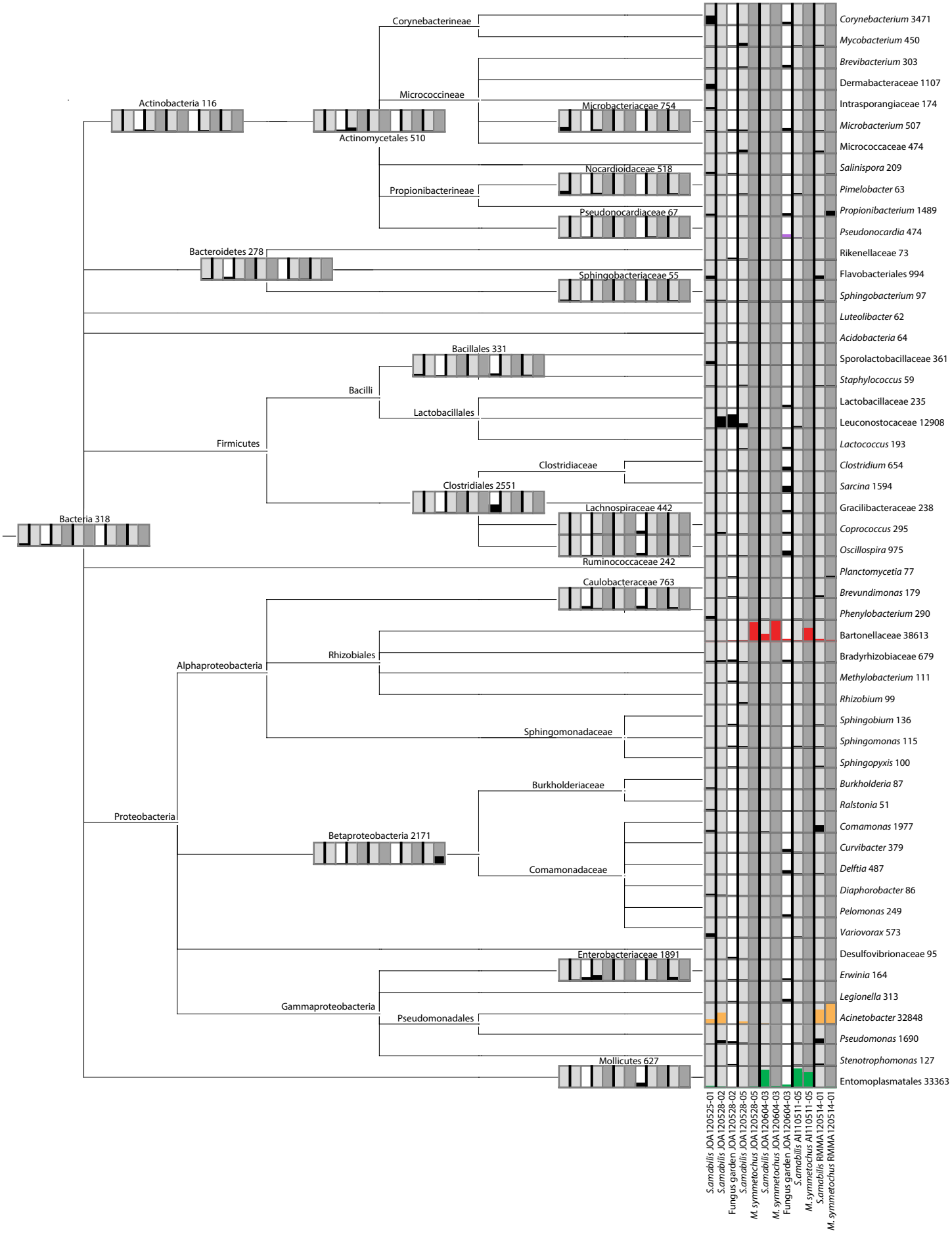
Bacteria 318
Actinobacteria 116
Actinomycetales 510
Corynebacterineae
Micrococcineae
Microbacteriaceae 754
Nocardioidaceae 518
Propionibacterineae
Pseudonocardiaceae 67
Bacteroidetes 278
Sphingobacteriaceae 55
Firmicutes
Bacilli
Bacillales 331
Lactobacillales
Clostridiales 2551
Clostridiaceae
Lachnospiraceae 442
Ruminococcaceae 242
Proteobacteria
Alphaproteobacteria
Caulobacteraceae 763
Rhizobiales
Sphingomonadaceae
Betaproteobacteria 2171
Burkholderiaceae
Comamonadaceae
Gammaproteobacteria
Enterobacteriaceae 1891
Pseudomonadales
Mollicutes 627
Corynebacterium 3471
Mycobacterium 450
Brevibacterium 303
Dermabacteraceae 1107
Intrasporangiaceae 174
Microbacterium 507
Micrococcaceae 474
Salinispora 209
Pimelobacter 63
Propionibacterium 1489
Pseudonocardia 474
Rikenellaceae 73
Flavobacteriales 994
Sphingobacterium 97
Luteolibacter 62
Acidobacteria 64
Sporolactobacillaceae 361
Staphylococcus 59
Lactobacillaceae 235
Leuconostocaceae 12908
Lactococcus 193
Clostridium 654
Sarcina 1594
Gracilibacteraceae 238
Coprococcus 295
Oscillospira 975
Planctomycetia 77
Brevundimonas 179
Phenylobacterium 290
Bartonellaceae 38613
Bradyrhizobiaceae 679
Methylobacterium 111
Rhizobium 99
Sphingobium 136
Sphingomonas 115
Sphingopyxis 100
Burkholderia 87
Ralstonia 51
Comamonas 1977
Curvibacter 379
Delftia 487
Diaphorobacter 86
Pelomonas 249
Variovorax 573
Desulfovibrionaceae 95
Erwinia 164
Legionella 313
Acinetobacter 32848
Pseudomonas 1690
Stenotrophomonas 127
Entomoplasmatales 33363
S.amabilis JOA120525-01
S.amabilis JOA120528-02
Fungus garden JOA120528-02
S.amabilis JOA120528-05
M.symmetochus JOA120528-05
S.amabilis JOA120604-03
M.symmetochus JOA120604-03
Fungus garden JOA120604-03
S.amabilis AI110511-05
M.symmetochus AI110511-05
S.amabilis RMMA120514-01
M.symmetochus RMMA120514-01

Fig. S6 Taxonomic assignment of 454 16S rRNA gene amplicons of *Sericomyrmex amabilis* hosts, *Megalomyrmex symmetochus* guest ants, and their fungus gardens as produced by MEGAN4 (Huson *et al.* 2011). Light grey cells represent host samples, dark grey cells are guest ant samples, and white cells are fungus garden samples, and the degree to which individual cells are filled with black or color represents the square-root of the number of reads of each phylotype in each sample. Ant and garden samples are ordered by nest ID, first the two guest ant-free host colonies and then the four pairs of guest ant-infected host colonies with samples belonging to different nests separated by vertical lines. As in Fig. 3, the Entomoplasmatales are plotted in green, Bartonellaceae in red, *Acinetobacter* in orange and *Pseudonocardia* in purple, whereas all other bacterial lineages are plotted in black. The total number of assigned reads per phylotype across the twelve samples is given behind the taxonomic assignment. Only OTUs with ≥ 50 reads were used to generate this plot and were then lumped into phylotypes.

Fig. S7

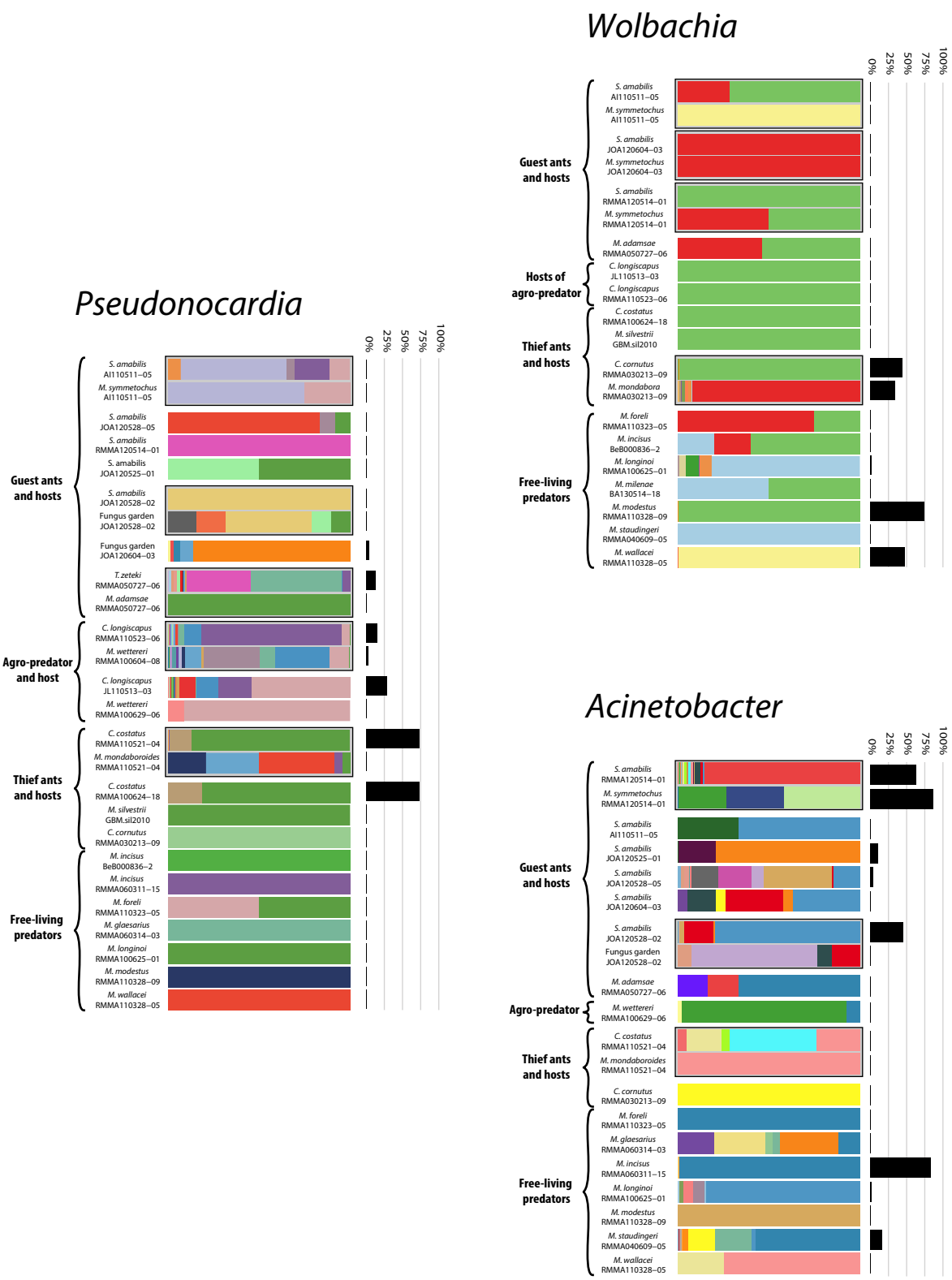
Wolbachia
0%
25%
50%
75%
100%
Guest ants and hosts
S. amabilis AI110511–05
M. symmetochus AI110511–05
S. amabilis JOA120604–03
M. symmetochus JOA120604–03
S. amabilis RMMA120514–01
M. symmetochus RMMA120514–01
M. adamsae RMMA050727–06
Hosts of agro-predator
C. longiscapus JL110513–03
C. longiscapus RMMA110523–06
Thief ants and hosts
C. costatus RMMA100624–18
M. silvestrii GBM.sil2010
C. cornutus RMMA030213–09
M. mondabora RMMA030213–09
Free-living predators
M. foreli RMMA110323–05
M. incisus BeB000836–2
M. longinoi RMMA100625–01
M. milenae BA130514–18
M. modestus RMMA110328–09
M. staudingeri RMMA040609–05
M. wallacei RMMA110328–05
Pseudonocardia
0%
25%
50%
75%
100%
Guest ants and hosts
S. amabilis AI110511–05
M. symmetochus AI110511–05
S. amabilis JOA120528–05
S. amabilis RMMA120514–01
S. amabilis JOA120525–01
S. amabilis JOA120528–02
Fungus garden JOA120528–02
Fungus garden JOA120604–03
T. zeteki RMMA050727–06
M. adamsae RMMA050727–06
Agro-predator and host
C. longiscapus RMMA110523–06
M. wettereri RMMA100604–08
C. longiscapus JL110513–03
M. wettereri RMMA100629–06
Thief ants and hosts
C. costatus RMMA110521–04
M. mondaboroides RMMA110521–04
C. costatus RMMA100624–18
M. silvestrii GBM.sil2010
C. cornutus RMMA030213–09
Free-living predators
M. incisus BeB000836–2
M. incisus RMMA060311–15
M. foreli RMMA110323–05
M. glaesarius RMMA060314–03
M. longinoi RMMA100625–01
M. modestus RMMA110328–09
M. wallacei RMMA110328–05
Acinetobacter
0%
25%
50%
75%
100%
Guest ants and hosts
S. amabilis RMMA120514–01
M. symmetochus RMMA120514–01
S. amabilis AI110511–05
S. amabilis JOA120525–01
S. amabilis JOA120528–05
S. amabilis JOA120604–03
S. amabilis JOA120528–02
Fungus garden JOA120528–02
M. adamsae RMMA050727–06
Agro-predator
M. wettereri RMMA100629–06
Thief ants and hosts
C. costatus RMMA110521–04
M. mondaboroides RMMA110521–04
C. cornutus RMMA030213–09
Free-living predators
M. foreli RMMA110323–05
M. glaesarius RMMA060314–03
M. incisus RMMA060311–15
M. longinoi RMMA100625–01
M. modestus RMMA110328–09
M. staudingeri RMMA040609–05
M. wallacei RMMA110328–05

Fig. S7 Distribution of 16S rRNA genotypes as identified by Oligotyping from the 454 16S rRNA pyrosequencing dataset based on all reads identified as *Pseudonocardia*, *Wolbachia* and *Acinetobacter*. As in Fig. 5, colors in the stacked bars represent the relative proportions of the different genotypes found in each sample, while black bar charts show the overall abundance of the specific bacterial lineages relative to the total microbiota in each sample, and boxes with black outlines highlight samples that were collected from the same nest. The number of reads per sample of all genotypes identified are given in Table S5, Supporting information.

Fig. S8 *Wolbachia wsp* gene

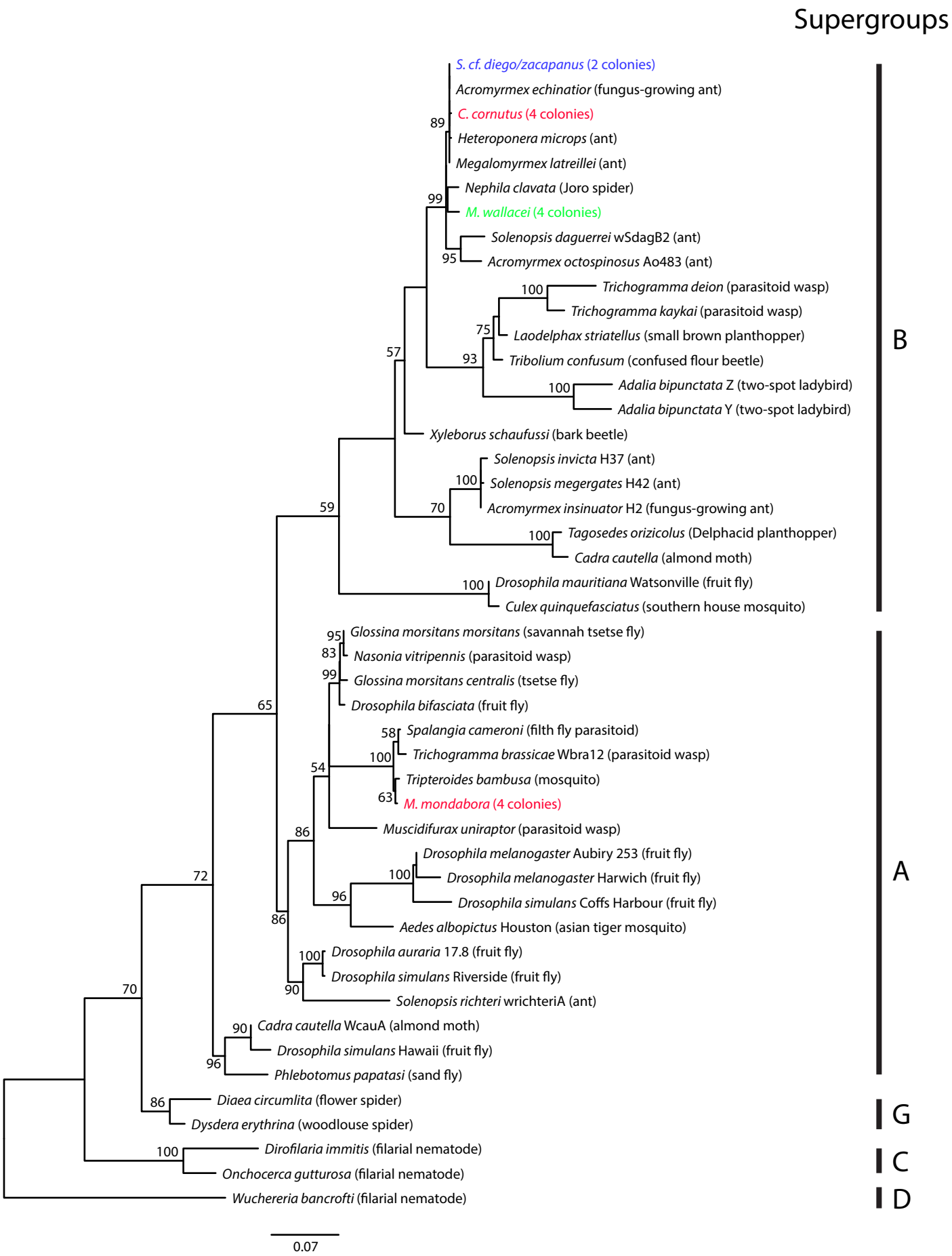

Fig. S8 Maximum Likelihood phylogeny based on ca. 520 bp of the *Wolbachia wsp* gene from a subsample of positive PCRs in our diagnostic screening, aligned with closely related sequences obtained from GenBank. Sequences from this study are colored according to the specific host-parasite associations and free-living *Megalomyrmex* as in Fig. 1, while sequences obtained from GenBank are shown in black. Values above the nodes represent support ≥ 50 after 1,000 bootstrap replicates.

Fig. S9

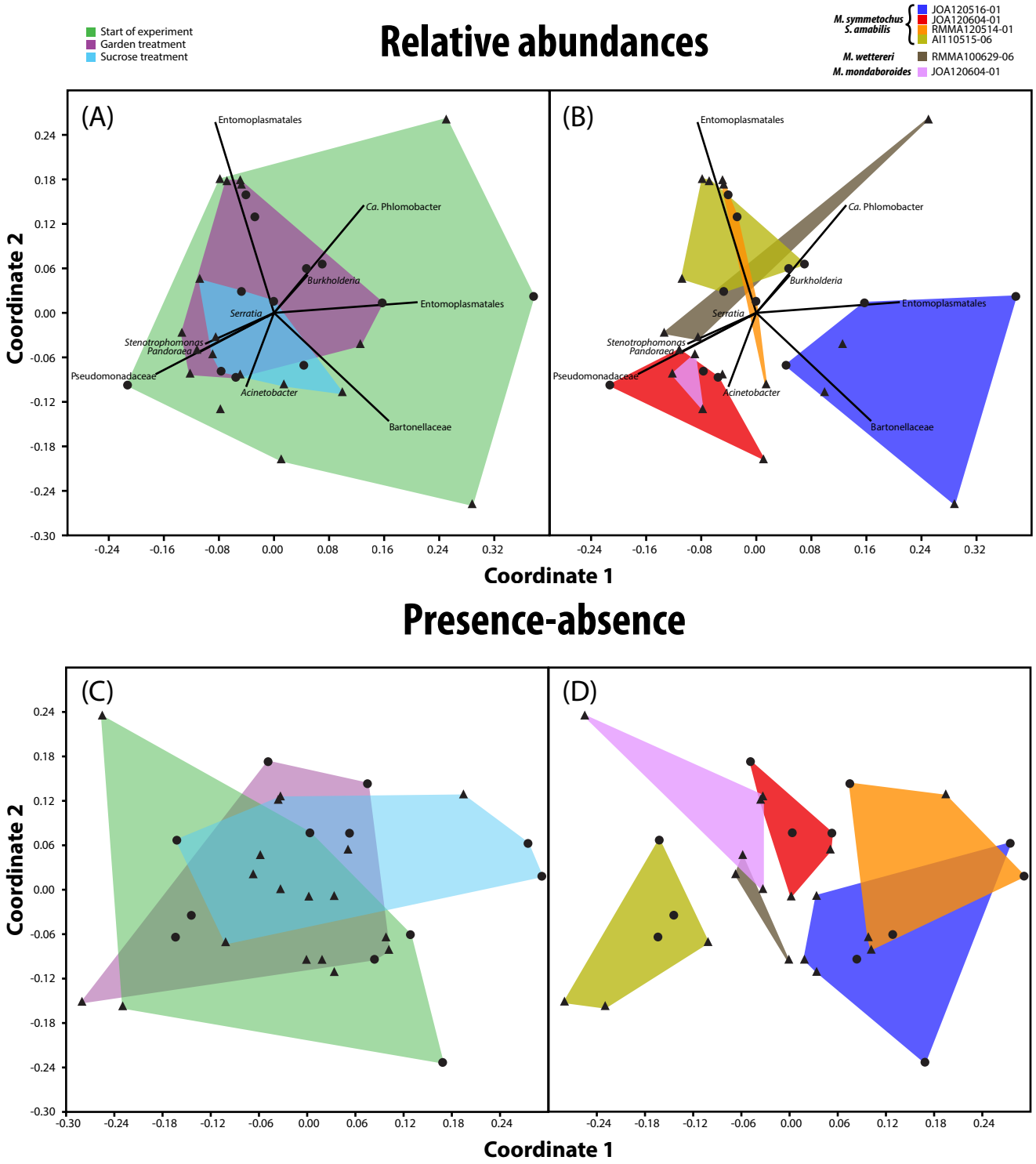
Relative abundances
Start of experiment
Garden treatment
Sucrose treatment
M. symmetochus
S. amabilis
JOA120516-01
JOA120604-01
RMMA120514-01
AI110515-06
M. wettereri
RMMA100629-06
M. mondaboroides
JOA120604-01
(A)
(B)
Entomoplasmatales
Ca. Phlomobacter
Burkholderia
Entomoplasmatales
Serratia
Stenotrophomonas
Pandoraea
Pseudomonadaceae
Acinetobacter
Bartonellaceae
Coordinate 2
Coordinate 1
Presence-absence
(C)
(D)

Fig. S9 Non-metric multidimensional scaling of Bray-Curtis dissimilarities between the bacterial communities identified in the diet manipulation experiment samples, calculated in two separate analyses from a matrix of relative abundances (A and B) and from a presence-absence matrix (C and D). *Megalomyrmex* social parasites are shown as triangles and hosts as circles. Black lines show the ten OTUs that had the strongest associations with the ordination axes in the weighted analysis (A and B), with the lengths and angles of the lines representing correlations between these OTUs and the axes. The plots of the two analyses were each split in two to show either the areas of occupancy of samples belonging to the different treatment groups (A and C) or the areas occupied by samples belonging to the different nests (B and D). Color-legends are given towards the upper left (for panels A and C) and the upper right (for panels B and D).